

Research  
Report**Smoke Reduction Methods Using Shallow-Dish Combustion Chamber in an HSDI Common-Rail Diesel Engine**

Yoshihiro Hotta, Kiyomi Nakakita, Takayuki Fuyuto, Minaji Inayoshi

**小型高速コモンレールディーゼル機関の浅皿型燃焼室による  
スモーク低減**

堀田義博，中北清己，冬頭孝之，稲吉三七二

**Abstract**

The cause of exhaust smoke from a small DI Diesel engine having small-orifice-diameter nozzles and a common-rail F.I.E. under the high-speed and high-load condition was investigated. In addition, methods by which to reduce this exhaust smoke were explored. Exhaust emission tests, in-cylinder observations and three-dimensional numerical analyses were performed. The following points were clarified during this study.

Under the abovementioned conditions, fuel

sprays are easily conveyed to the squish area by a strong reverse squish. Therefore, the air in the piston cavity is not used effectively. Suppressing the airflow in the piston cavity by using a shallow-dish type combustion chamber decreases the excessive outflow of the fuel-air mixture into the squish area and allows full use of the air in the piston cavity. Hence, the exhaust smoke is reduced. This results in increased specific power, which is limited by the amount of exhaust smoke.

**Keywords** Diesel engine, HSDI, Shallow-dish chamber, Common-rail, Specific power

**要 旨**

小型高速コモンレールディーゼル機関に小噴孔径ノズルを用いた際の、高速高負荷におけるスモーク増加要因を解析し、その低減策を探索した。排気試験、筒内観察、3次元数値シミュレーション手法を用い、以下の結論を得た。上記の運転条件では、燃料噴霧は激しい逆スキッシュ流によりスキッシュエリアに運ばれる。このた

め、ピストンキャビティ内の空気が十分に利用されない。浅皿型燃焼室によりピストンキャビティ内の気流を抑制することで燃料蒸気がスキッシュエリアに過剰に吹きこぼれなくなり、ピストンキャビティ内の空気が十分に利用されるようになる。これによりスモークが低減され、スモーク排出量によって制限される出力が向上する。

**キーワード** ディーゼルエンジン，HSDI，浅皿型燃焼室，コモンレール，比出力

## 1. Introduction

During the recent development of small HSDI (High-Speed Direct Injection) Diesel engines, increasing the specific power is an important issue. One important step to realize this is decreasing the exhaust smoke under the high-speed condition, because the maximum torque is generally limited by the amount of exhaust smoke. Therefore, in general, the combination of relatively large-diameter nozzles and deep-bowl type combustion chambers has been used in recent years for small HSDI Diesel engines, due to its short injection period and strong fuel-air mixing effect.

On the other hand, in order to meet present and future stringent emission standards, it is necessary to use a moderate small-orifice-diameter nozzle and a common-rail fuel injection system that enables high flexibility in adjusting injection parameters, such as pressure and timing.<sup>1, 2)</sup> However, for the conventional deep-bowl type combustion chamber, the combination of a small-orifice diameter nozzle and a common-rail injection system is likely to increase the exhaust smoke under high-speed and high-load conditions. This study attempts both to clarify the cause of high levels of exhaust smoke under the abovementioned conditions and to provide countermeasures against that. The application of effective countermeasures is expected to enable the realization of high specific power while maintaining low exhaust emissions.

## 2. Experimental apparatus and the calculation model

### 2.1 Engine specifications

The level of exhaust smoke and the combustion characteristics of the HSDI common-rail Diesel engine were examined using a single-cylinder research engine. Next, the combustion processes were observed using an optically accessible engine. The bore and stroke were the same for both engines. The specifications of these engines are listed in **Table 1**. An external supercharging apparatus was used to simulate turbo charging.

A nozzle orifice diameter of 0.17 mm was selected as being representative of recent conventional nozzles for this displacement volume class of HSDI

Diesel engine, and a nozzle orifice diameter of 0.14 mm was selected as being representative of an advanced small-orifice-diameter nozzle for further reducing emissions. Both nozzles were of the six-orifice VCO type. Hereafter, these nozzles shall be referred to as the 0.17-nozzle and the 0.14-nozzle, respectively. The nozzle cone angle is 150 degrees, unless otherwise noted.

### 2.2 Experimental conditions

An engine speed of 4000 rpm was selected as the typical high-speed condition, and an engine speed of 2000 rpm was selected as the typical medium-speed condition. The experimental conditions are listed in **Table 2**. The level of exhaust smoke was compared for the same injection quantity. Fuel injection timing was selected such that the torque was maximized under a limited maximum cylinder pressure of 15 MPa.

### 2.3 Three-dimensional CFD

The airflow motion and fuel-air mixture formation processes were calculated based on the KIVAII code.

**Table 1** Engine specifications.

Bore × Stroke	83mm × 92mm
Displacement	497.8 cm <sup>3</sup>
Compression Ratio	18.8
Port Swirl Ratio	2.3
Layout of Valves & Injector	2-Inlet 2-Exhaust Center Injection
Fuel Injection System	Common Rail

**Table 2** Experimental conditions.

Engine Speed rpm		2000	4000
Common Rail Press. MPa		90	130
Fuel Injection Amount mm <sup>3</sup> /st		55	50
Injection Timing deg.ATDC (Duration CA)	φ 0.17	-1 (16.2)	-6 (27.5)
	φ 0.14	-3 (22.3)	-7 (35.8)
Charging Efficiency %		180	170
Equivalence Ratio		0.64	0.62

The spray model used in this study is the Hybrid breakup model.<sup>3)</sup> The model was modified with respect to the breakup parameter and the droplet size distribution.

### 3. Combustion processes and cause of exhaust smoke under high-speed and high-load condition

#### 3.1 Exhaust emissions and combustion characteristics

A comparison of the exhaust smoke between the 0.17-nozzle and the 0.14-nozzle is shown in **Figs. 1(a)** and **(b)** for 2000 rpm and 4000 rpm, respectively. Here, the deep-bowl type combustion chamber was employed, which is representative of conventional chambers used in recent DI Diesel engines of this class. For this combustion chamber, the aspect ratio is 2.8, and the maximum diameter is 43 mm.

At 2000 rpm, the levels of exhaust smoke produced by the two nozzles were almost identical. However, at 4000 rpm, the level of exhaust smoke was markedly higher for the 0.14-nozzle engine as compared to the 0.17-nozzle engine.

#### 3.2 Combustion processes with the small-orifice-diameter nozzle under the high-speed and high-load condition

The combustion processes at 2000 rpm and 4000 rpm were examined using both the conventional 0.17-nozzle and the 0.14-nozzle. The results of this examination are shown in the four left-most columns of **Fig. 2**. Based on these results, the following points were clarified.

For the 0.17-nozzle at 2000 rpm, the fuel sprays progress in a straight line without being deflected by the swirl due to the strong penetration of the fuel

spray (-0.2 deg.ATDC). Thus all of the flame jets impinge significantly onto the chamber wall and are well mixed with ambient air (3.4 deg.ATDC). Then, the dark brown area appears on the bottom window. This indicates that flame jets successfully develop to the bottom of the piston cavity. The above combustion processes are schematically summarized in **Fig. 3(a)**. The squish flow and the fuel jet generate vertical flow. The combination of the vertical flow and swirl flow then forms a spiral vortex. This complicated flow pattern is considered to contribute to the promotion of soot oxidization.

For the 0.14-nozzle at 2000 rpm, the characteristics of the combustion processes are almost identical to those of the 0.17-nozzle. The same complicated flow pattern of the spiral vortex as in the case of the 0.17-nozzle is observed.

However, at 4000 rpm, a significant difference appears between the 0.17-nozzle and the 0.14-nozzle. For the 0.17-nozzle, flame jets successfully impinge on the chamber wall and then develop to the bottom of the cavity. This flame development is confirmed by the dark brown soot areas on the observation window at 22.8 deg.ATDC. Thus, the spiral vortex flow shown in **Fig. 3(a)** is also observed for this case. In contrast, for the 0.14-nozzle at 4000 rpm, the fuel sprays are strongly deflected by the swirl before reaching the chamber wall (1.8 deg.ATDC). As a result, unlike the other cases, the flame jets fail to develop to the bottom of the cavity. This difference occurs because, at this high engine speed, the momentum of the fuel spray of the 0.14-nozzle is relatively weak compared to the airflow.

A comparison of the flame development into the squish area at the latter part of the combustion period is shown in the four left-most columns of **Fig. 4**. At 2000 rpm, the main part of the luminous flame exists inside of the cavity for both nozzles. However, at 4000 rpm, a large amount of luminous flame blows out to the squish area, especially for the 0.14-nozzle.

**Figure 5** shows a comparison of the fuel vapor distribution between the 2000 rpm and 4000 rpm engine speeds calculated using 3D-CFD for the 0.14-nozzle. At 2000 rpm, the fuel vapor exists both in the cavity and in the squish area. However, at

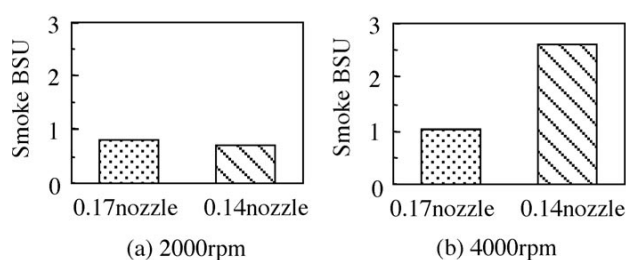


**Fig. 1** Comparison of exhaust smoke.

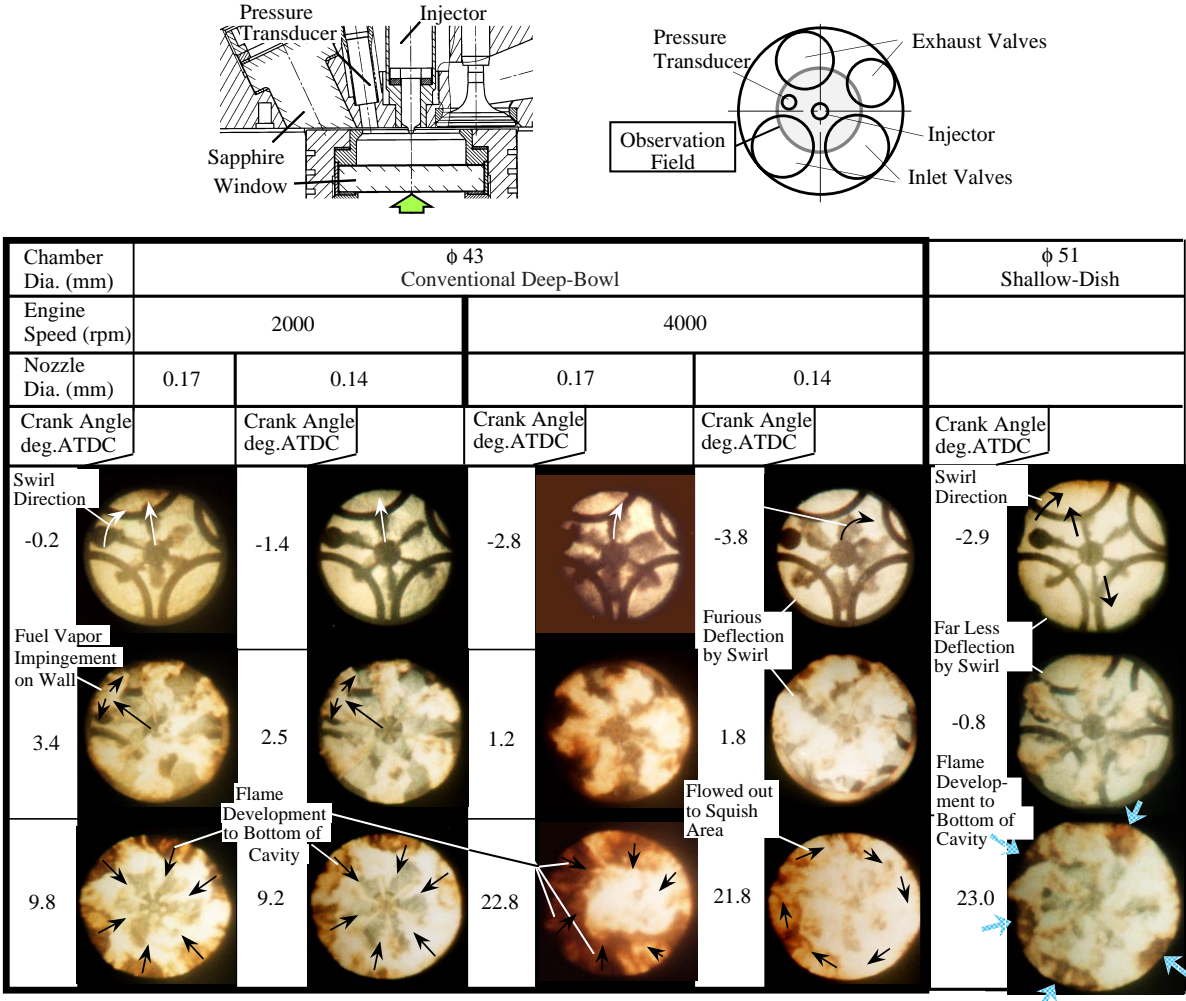


Fig. 2 Comparison of combustion process.

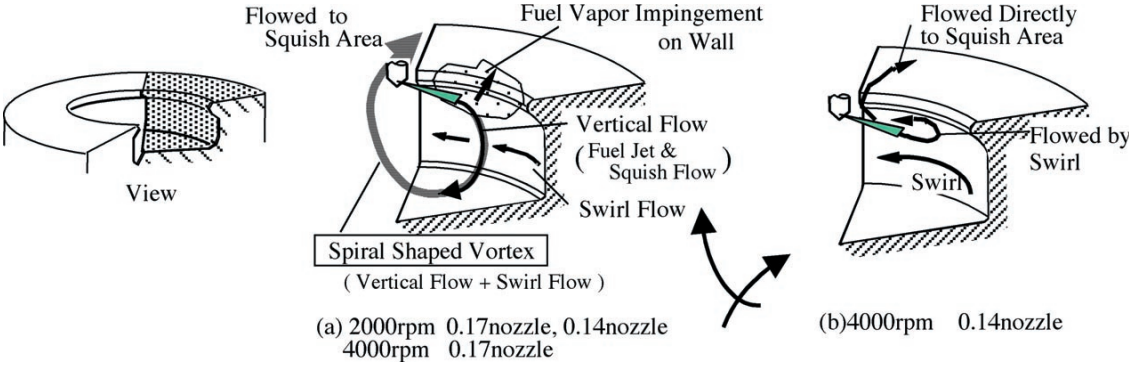


Fig. 3 Schematic diagram of flame development in combustion chamber.



4000 rpm, almost all of the fuel vapor blows out to the squish area. Thus, the air in the cavity is not fully used to oxidize the fuel.

Based on these results, the combustion processes for the 0.14-nozzle at 4000 rpm are summarized in Fig. 3(b). The promotion of fuel-air mixing by spray-wall impingement is slight because the fuel sprays are highly deflected by a strong swirl. Thus, the air in the cavity cannot be fully used because the fuel vapor is conveyed to the squish area by a strong reverse squish flow.

#### 4. Smoke reduction methods using the shallow-dish combustion chamber

##### 4.1 Reduction of exhaust smoke by enlarging combustion chamber diameter

Based on the above results, the effect of suppressing strong airflow by enlarging the combustion chamber diameter is examined.

The evaluated combustion chambers are shown in Fig. 6. The aspect ratio was increased to 5.2 from 2.8 in the earlier investigation, while maintaining the same compression ratio. An approximately 40% suppression of both the cavity swirl ratio and the squish velocity is realized by enlarging the diameter

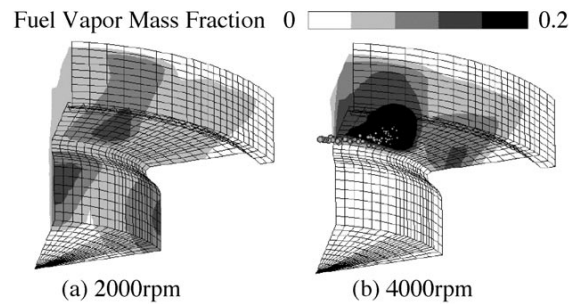


Fig. 5 Computational analysis of mixture distribution.

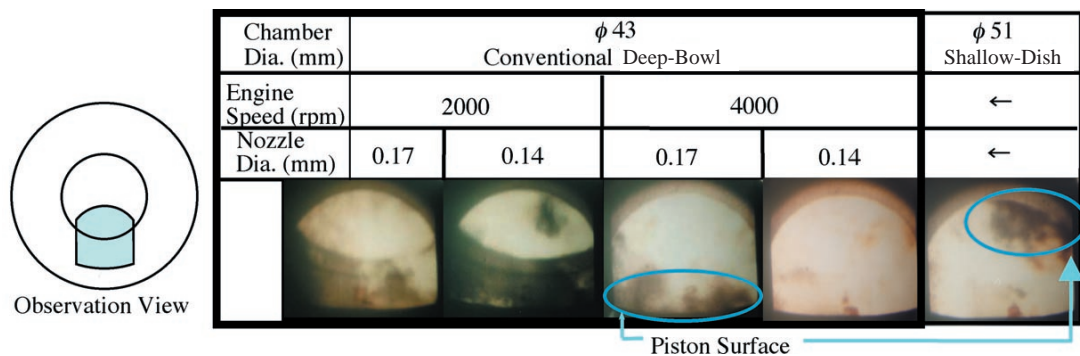


Fig. 4 Comparison of flame development in squish area (35 deg. ATDC).

Chamber Diameter (mm)	$\phi 43$	$\phi 47$	$\phi 51$	$\phi 55$
Aspect Ratio	2.8	3.4	4.2	5.2
Schematic Chamber Configuration				

Fig. 6 Variation in combustion chamber.

of the chamber from  $\phi 43$  to  $\phi 55$ . For the sake of simplicity, hereinafter only the maximum chamber diameter is referenced to indicate these chambers, such as  $\phi 43$ -chamber and  $\phi 55$ -chamber.

The relations between the combustion chamber diameter and exhaust smoke at the high-load condition are shown in Fig. 7(a) for 2000 rpm and in Fig. 7(b) for 4000 rpm for both nozzle cases. The case of the expanded cone angle of 155 degrees for the 0.14-nozzle is also shown.

At 2000 rpm (Fig. 7(a)), a change in the nozzle orifice diameter in the examined range does not affect the characteristics of the exhaust smoke with respect to the chamber diameter, so long as the same nozzle cone angle is used. Namely, for both nozzle diameters, the exhaust smoke is minimized by the  $\phi 47$ -chamber and is drastically increased by enlarging the chamber diameter.

On the other hand, at 4000 rpm, the minimum exhaust smoke level is obtained at different chamber diameters for different nozzles, as shown in Fig. 7(b). For the 0.17-nozzle, the  $\phi 47$ -chamber produces minimum smoke, as is the case at 2000 rpm. However, for the 0.14-nozzle, the minimum smoke level is obtained for the  $\phi 51$ -chamber. Thus, for the high-speed and high-load condition, the optimum diameter of the combustion chamber increases with decreasing nozzle hole diameter.

In addition, at 4000 rpm, the exhaust smoke produced by the  $\phi 51$ -chamber using the 155-degree /0.14-nozzle is almost equivalent to that using the

150-degree/0.14-nozzle. Thus, low levels of exhaust smoke can be realized at 2000 rpm (Fig. 7(a)) and 4000 rpm (Fig. 7(b)) by the 155-degree/0.14-nozzle and the  $\phi 51$ -chamber combination.

#### 4.2 Combustion processes of the shallow-dish combustion chamber

The combustion processes of the shallow-dish type  $\phi 51$ -chamber were examined at 4000 rpm using the 0.14-nozzle. The observation results of the combustion chamber and the squish area are shown respectively in the right-hand column of Fig. 2 and the right-hand column of Fig. 4.

Here, the fuel sprays are only slightly deflected by the swirl flow and progress in an almost straight line, as shown in the two top-most photographs in the right-hand column of Fig. 2. Then, the dark brown areas are produced on the bottom glass at 23.0 deg. ATDC. This indicates that the flame jets successfully develop to the bottom of the cavity and that the air at the bottom of the combustion chamber is used effectively. In the visualization from the top (Fig. 4, right-hand column), the amount of luminous flame blowing out of the piston chamber is suppressed by the use of the  $\phi 51$ -chamber.

#### 4.3 3D-CFD numerical analysis

The fuel-air mixture distribution and airflow patterns in the conventional deep-bowl type  $\phi 43$ -chamber and shallow-dish type  $\phi 51$ -chamber are calculated at 4000 rpm for the 0.14-nozzle. The results are shown in Fig. 8 and Fig. 9, respectively.

For the  $\phi 43$ -chamber, almost all of the fuel-air

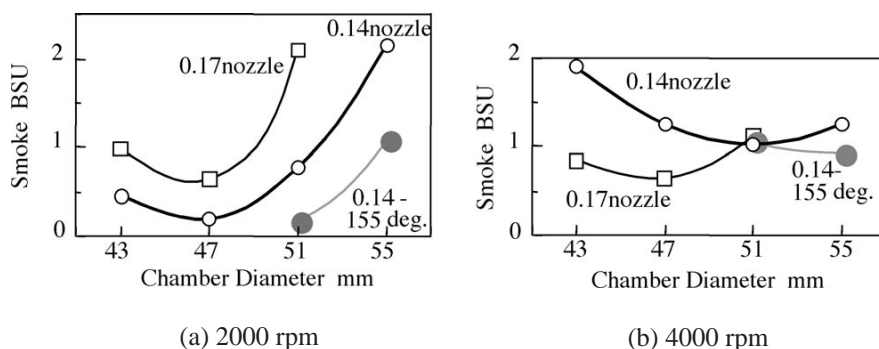


Fig. 7 Effect of chamber diameter on exhaust smoke.

mixture flows out to the squish area, as shown in Fig. 8. This could be due to not only the high velocity of the reverse squish but also its nearly vertical upward direction, which are shown as small vector arrows in the left figure of Fig. 9. This upward flow is considered to strongly convey the fuel vapor out into the squish area from the cavity.

On the other hand, for the shallow-dish type  $\phi 51$ -chamber, the velocity of the reverse squish is lower than that of the  $\phi 43$ -chamber, and the cross-angle between the fuel spray and the reverse squish flow is narrower, as shown in Fig. 9. In addition, the

geometric impinging point of the fuel spray onto the chamber wall is lower than that of the  $\phi 43$ -chamber. Therefore, the fuel-spray can enter the cavity, and the air in the cavity is used effectively, as shown in Fig. 8.

## 5. Conclusion

(1) The combination of a conventional deep-bowl type combustion chamber, a small-orifice-diameter nozzle and a common-rail fuel injection system increases the exhaust smoke under the high-speed and high-load condition, resulting in decreased specific power for the same smoke level. This phenomenon occurs due to significant amounts of fuel sprays being conveyed to the squish area by the strong reverse squish flow of the deep-bowl combustion chamber, because the momentum of the fuel sprays is relatively small compared to the well-developed airflow.

(2) The high level of exhaust smoke produced by a small-orifice-diameter nozzle and a common-rail fuel injection system under the high-speed and high-load condition can be suppressed by introducing a shallow-dish type combustion chamber. A reduced amount of fuel-air mixture is conveyed to the squish area due to the reduced velocity and inclined direction of the reverse squish, and due to the downward shift of the geometric spray-wall impinging point inside of the cavity. Therefore, realization of full use of the air in the piston cavity allows the specific power to be increased for a limited level of exhaust smoke.

## Acknowledgement

This research was supported by Toyota Motor Corporation.

## References

- 1) Nakakita, K., et al. : Trans. Jpn. Soc. Mech. Eng., Ser. B, **60**-577(1994), 3198-3206
- 2) Schommers, J., Duvinage, F., et al. : SAE Tech. Pap. Ser., No.2000-01-0944, (2000)
- 3) Beatrice, C., Belardini, P., et al. : SAE Tech. Pap. Ser., No. 950086, (1995)

( Report received on July 10, 2002)

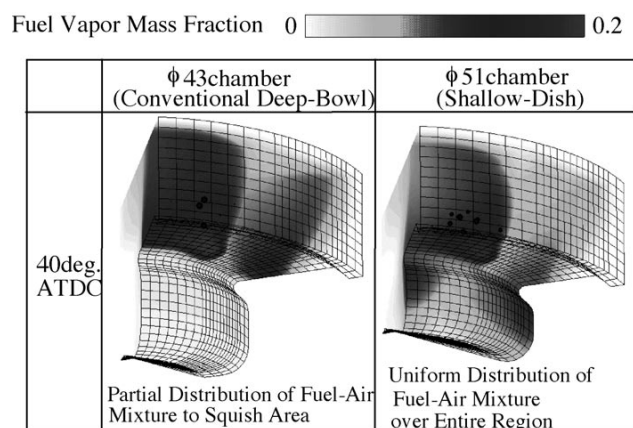


**Fig. 8** Computational analysis of mixture distribution for each chamber (Engine speed = 4000 rpm, 0.14-nozzle).

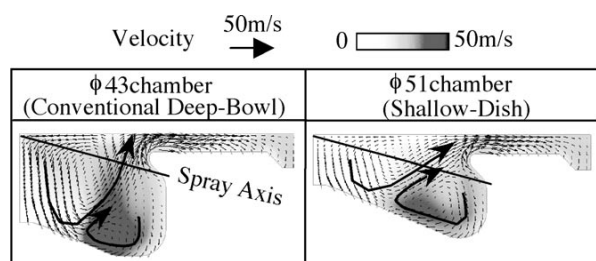


**Fig. 9** Simulated flow patterns for each chamber at 14 deg. ATDC (without fuel spray, Engine speed = 4000 rpm).


**Yoshihiro Hotta** 堀田義博

Year of birth : 1968  
 Division : Research-Domain 11  
 Research fields : Diesel engine combustion  
 Academic society : The Soc. of Autom.  
 Eng. of Jpn., The Jpn. Soc. of  
 Mech. Eng.


**Takayuki Fuyuto** 冬頭孝之

Year of birth : 1971  
 Division : Research-Domain 11  
 Research fields : Diesel engine combustion  
 Academic society : The Soc. of Autom.  
 Eng. of Jpn., The Jpn. Soc. of  
 Mech. Eng.


**Kiyomi Nakakita** 中北清己

Year of birth : 1952  
 Division : Research-Domain 11  
 Research fields : Diesel engine combustion  
 Academic degree : Dr. Eng.  
 Academic society : The Soc. of Autom.  
 Eng. of Jpn., The Jpn. Soc. of  
 Mech. Eng., Combustion Soc. of  
 Jpn., Inst. for Liq. Atomization and  
 Spray Systems - Jpn.  
 Awards : The outstanding tech. pap.  
 award, The Soc. of Autom. Eng. of  
 Jpn., 1992 & 2000.  
 Engine Systems Memorial Award,  
 The Engine Systems Div., The Jpn.  
 Soc. of Mech. Eng., 1996.


**Minaji Inayoshi** 稲吉三七二

Year of birth : 1952  
 Division : Research-Domain 11  
 Research fields : Diesel engine combustion